SLAC-PUB-6559
June 1994
(A)

Proposed Emittance Upgrade for the SLC Damping Rings*

R.Early,T.Limberg,H.Moshammer,T.Raubenheimer, K.Skarpaas, J. Spencer and SLAC MMG+
Stanford Linear Accelerator Center, Stanford University
Stanford, California 94309

Abstract: One way to improve luminosity is to reduce transverse emittance by changing damping partitions. We consider the options in relation to the constraints. Besides modifications of the basic DR configuration the options include closed-orbit offsets in the quadrupoles, addition of strong multipoles and replacement of existing rectangular nosepieces on the dipoles (shim angles $\phi \equiv \theta/2$) with rotatable inserts. Measurements indicate the possibility of dynamically tuning $\phi \geq 45°$ with decreases in τ_x and ϵ_x of ≥50%. We discuss damping mechanisms to motivate the desirable field characteristics as well as nonlinear contours to cancel dipole harmonic errors (B>2T here) or to provide chromatic corrections. Such inserts could also be used to make cheaper, more compact rings with better impedance by reducing the number of conventional multipoles without impairing the stability. Estimated hardware costs are 250$/dipole end or multipole equivalent.

1. Introduction

Rings such as the SLC DRs[1] are an underused resource that need more study for current uses and other possibilities such as 'parasitic' radiation sources. For colliders they provide natural boundaries or 'treaty points' crucial for synchronization and feedback. Optimal, stable injection and extraction of beams into or out of these rings and the dynamic tuning of characteristics such as the emittance or phase-space distribution are important, related questions.

Because emittance growth in the SLC linac and arcs is not matched to the DR's, luminosity gains are possible by reducing the transverse emittance from the rings. In Ref. [2], we reduced the emittance by a factor of three by designing new bending magnets that changed the damping partitions and decreased dispersion. Here we consider the less invasive and less expensive approach of decreasing emittance by only changing the damping partitions.

The equilibrium horizontal emittance ϵ_x scales inversely with the horizontal damping partition J_x which is normally close to 1. The allowable change in J_x is limited by the longitudinal emittance of the extracted beam. Robinson's Theorem showed that increasing the horizontal damping decreases the longitudinal. In the SLC, we cannot increase J_x by more than 80% because of constraints on the longitudinal emittance ϵ_E.

*Work supported by Department of Energy contract DE-AC03-76SF00515.

+ The authors thank the Magnetic Measurements Group.

2. The Current System without Errors

The 'definitions' of damping partitions J_i, ϵ_i & τ_i are given in terms of the synchrotron integrals[3] in Table I. The calculations are based on actual field measurements such as shown in Fig. 1. Our goal was to modify I_4 without reducing I_2 significantly and thus worsen ϵ_y & τ_y.

We have compared a variety of measurements of the emittance and damping times to calculations that included errors such as random misalignments that produce dispersion [4]. These calculations gave reasonably good results that justifiy pursuing this work in terms of the integrals in Table I assuming, of course, that we can obtain matched solutions to the desired tunes that have good dynamic aperture.

3. Options for Modifying the Damping Partitions

It is clear from Fig. 1 that the dipole fringe fields extend far beyond the physical boundaries. The equivalent sector magnet with finite fringe fields (FFF) in Table I would have I_4=0.121 m^{-1} so we want to make the dipoles into reverse sector magnets i.e. add some equivalent defocusing quadrupole strength in this region. Strong permanent magnet defocusing quads (PMQD) inserted close to the main bending magnets (inside the permanent magnet sextupoles SD & SF [5] in Fig. 1) could then decrease I_4 and thus reduce the horizontal equilibrium emittance and damping time by a nearly equal amount.

Table I. Beam Parameters for an Error-Free Ring

Sharp CutOff vs Finite Fringe	SCOFF	FFF
$\alpha = \frac{1}{L}\oint G\eta ds$ [m^{-1}]	0.015	0.016
$I_2 = \oint G^2 ds$ [m^{-1}]	3.205	2.785
$I_3 = \oint G^3 ds$ [m^{-2}]	1.635	1.347
$I_4 = \oint (G^2 + 2K) G\eta ds$ [m^{-1}]	-0.006	-0.029
$I_5 = \oint G^3 H ds$ [m^{-1}]	0.0210	0.0175
$J_x = 1 - I_4/I_2$	1.00	1.01
$-dJ_x/d\delta$	15.0	16.5
$\epsilon_x \simeq \lambda_c \gamma^2 I_5/(J_x I_2)$ [nm]	13.7π	13.0π
$\sigma_E/E \simeq [\lambda_c \gamma^2 I_3/(J_E I_2)]^{\frac{1}{2}}$ [%]	0.073	0.071
τ_x [ms]	3.09	3.52
$\tau_y \propto T_o/I_2$ [ms]	3.09	3.56
τ_E [ms]	1.56	1.79

Presented at the Fourth European Particle Accelerator Conference (EPAC'94), London, England, June 27-July 1, 1994

We could also add permanent magnet multipoles (combined dipole/quadrupole magnets) around the ring including additional quads to avoid modifiying the primary DR quadrupoles. Notice that imposing an additional K value perturbs the tunes and may cause the primary DR focusing quads (QF) to run out of range when compensating for a negative K.

Introducing closed-orbit offsets in these primary quads is another variant that doesn't lead to tune changes but may cause stability problems. Finally, adding variable shim angles to the dipole ends is of interest because the dipoles in the DR FODO cells have removable pole ends at entrance and exit.

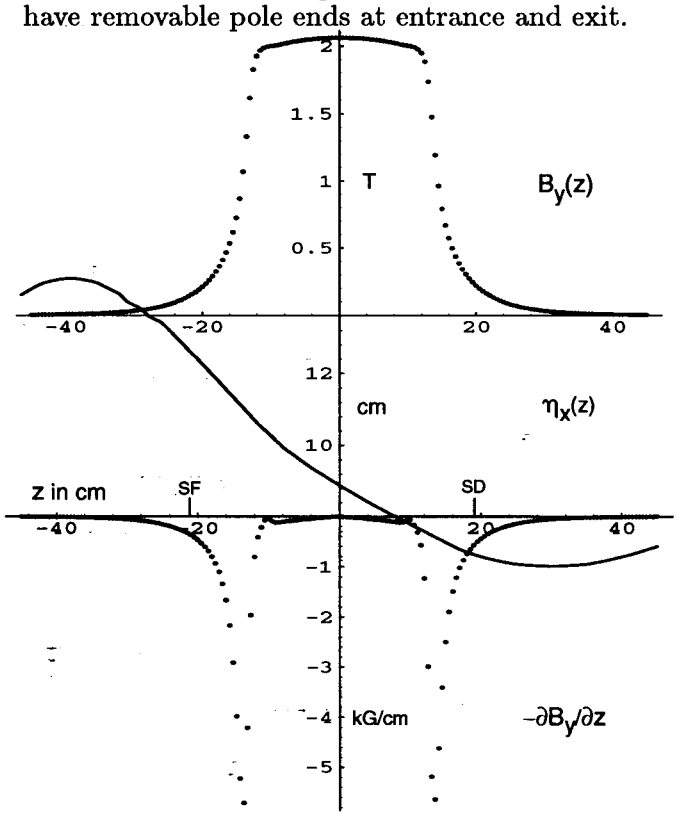

Fig. 1: Measured Dipole Data and the Design η_x.

5. Variable Pole Face Rotations

Rectangular dipoles have a total bend angle $\theta=\phi_i+\phi_o$ with parallel entrance and exit faces. Such magnets have the advantage that all high order, horizontal magnification terms are zero: $(x|x^n)=0$ for n>1 as well as many angular and chromatic terms e.g. $(\delta|x^n)$ for n>0 [6]. These are seldom considered in tracking codes. Assuming the isoinduction lines in the fringe fields are straight and parallel over several gaps outboard from the pole-face i.e. a pole width of several gaps, a simple pole face rotation by an angle ϕ is then expected to produce an effective quadrupole of strength:

$$K(s) = \frac{e}{p_o}\frac{dB_y(s)}{ds}\,tan(\phi)$$

where the last two terms are the gradient dB_y/dx. Fig. 1 shows the longitudinal gradient for these dipoles. Because the characteristic dimensions such as the dipole half gap, beam-stay-clear and other multipole radii are $\sim$ 1 cm here, such dipoles can generate strong quadrupole fields.

In the sharp cut off approximation (SCO) for the dipole field, $I_4 \rightarrow 0$ for rectangular dipoles with constant or linear variation in η because:

$$I_4 \propto <\eta>\theta - \eta_i tan(\phi_i) - \eta_o tan(\phi_o)\ .$$

This implies that we would like to minimize η in the center of the dipoles in the same way that we would like β_y to be small there. Alternatively, we can consider some form of combined function magnet as suggested above. Clearly, because $<\eta> \propto \alpha$, low momentum compaction rings are useful for this. Similarly, because of the higher tune required in the horizontal plane, we see from Fig. 1 that η is largest on the QF side rather than near the QDs where we would have preferred it for these purposes.

When we replace one rectangular endpiece on the dipoles with a rotatable, half-cylinder of permendur at -30° we obtain α=0.014, $\tau_{x,y,E}$=3.02,3.63,2.02 ms, σ_ϵ=0.074 % and ϵ_x=11.1 nm. This requires no other modifications to the ring. Fig. 2 compares the strength $\frac{p_o}{e}K(s)$ based on the longitudinal gradient from a single field scan at x,y=0 to dB_y/dx derived from maps such as used in Fig. 3. We begin to see the small size of the permendur (R=2.5 cm half cylinder) at this angle.

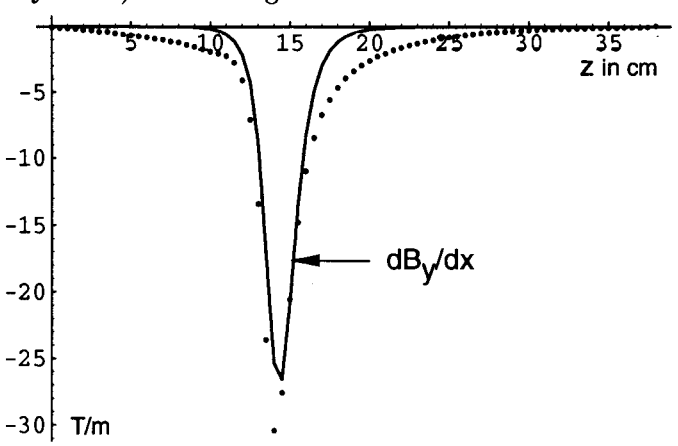

Fig. 2: Comparison of Gradient Models for ϕ=30°.

Comparison of data for the existing dipole (Fig. 1) to measurements made with the permendur at 0° shows that the longitudinal gradient $(\partial B_y/\partial z)^{max}_{x,y=o}$ increases and that its location is pushed outward. Further, this effect is magnified when a nonmagnetic shim is inserted between the pole and the endpiece. One expects some increase in the basic damping time τ_y from such effects but calculations show this is small (3.56→3.63 ms).

6. Addition of PM Multipoles

Three different locations of two permanent quads on either side of the dipoles were investigated. Their assumed lengths were 1 cm. Their distances from the center of the bends in the 3 cases were respectively: 14.5/15.5 cm, 15/16 cm and 16/17 cm whereas the yoke length is L_Y=30.5 cm and the pole length is L_P=29 cm. The existing parameters are in the first row of Table II below for comparison:

PMQD [kG/cm]	$\oint B_y ds$ [kG cm]	I_4 [1/m]	J_x	QF [1/m^2]	$\gamma\epsilon_x$ 10^{-5}m
		-0.01	1.00	18.4	3.19
-8.0/-8.0	9.7 / 6.5	-1.06	1.38	21.5	2.13
-10./-8.0	"	-1.22	1.44	21.9	2.04
-8.0/-8.0	8.12/ 5.65	-0.91	1.32	21.5	2.23
-9.6/-8.0	"	-1.01	1.36	21.8	2.16
-8.0/-8.0	5.65/ 4.19	-0.65	1.23	21.5	2.39
-10./-8.0	"	-0.73	1.26	21.8	2.32

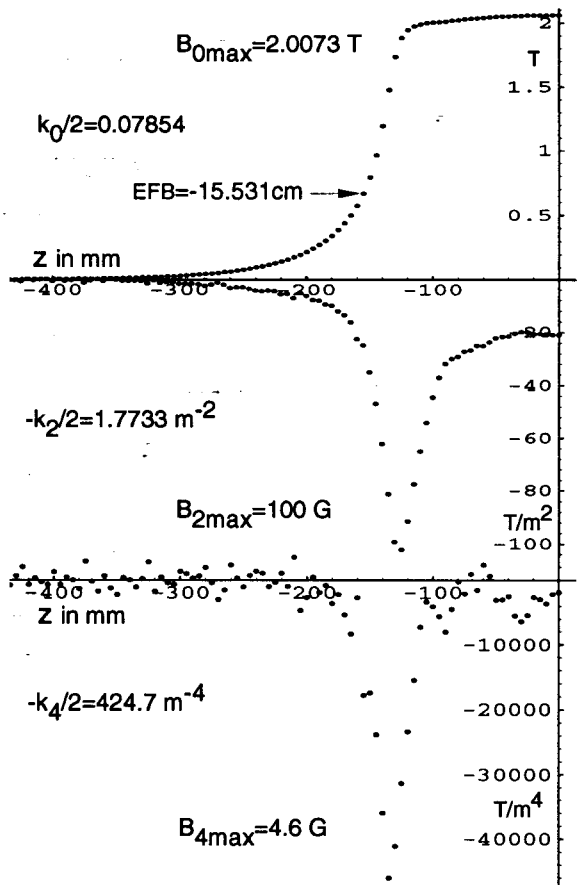

Fig. 3: $\frac{p_o}{e}K_n(z)$ Distribution of Allowed Multipoles.

The maximal strength of the QF and matching problems limit the reduction of the horizontal emittance. Due to the exponential drop of the fringing field, the gain depends crucially on how close to the bends the quads can be placed. Cases 2 & 3 were practical for the current pole length but their location was not compatible with the new vacuum chamber. The vertical chromaticity goes negative ($\xi_y \approx -0.4$) and would also need extra correction.

8. Higher Order Field Errors & Corrections

It is difficult to simulate the 3-D characteristics of magnets at high fields so it is prudent to allow for this with some dynamic tuning for compensation. A good example was discovered with the DR bends after a small energy increase. Fig. 3 shows the longitudinal distribution of multipole strengths from measurements made at the same time as those for Fig. 1. Only half a magnet is shown. One sees that these magnets were reasonably well designed in 2D because the body sextupole is less than the fringing field component and there is very little body decapole. Still, the integrated sextupole strength of a DR dipole is k_{2D}=-3.55 m^{-2} compared to a PMSD of k_{2SD}=-27.3 m^{-2}. This made the horizontal chromaticity nearly zero but can be compensated with a slight curvature to the permendur inserts.

9. Conclusions

If one perturbs the orbit or enlarges the ring, then according to Table I we can increase J_x by 10% or more but we also expect problems. Similarly, using strong PM magnets near strong dipoles also has problems. The preferred method, especially with removable nose pieces, is to use rotatable, vanadium permendur inserts that can also be used to locally compensate the observed sextupole component in these dipoles. Since RF $\vec{e}$ sources may ultimately allow us to bypass the e^- ring, it seems reasonable to first try these on the e^+ ring. From Table II and the η in Fig. 1 we expect almost 50% increases in J_x when we include these on the QF side of each dipole. Matched solutions with good dynamic aperture exist up to 45° but require QF modifications.

10. References

[1] G. Fisher, W. Davies-White, T. Fieguth and H. Wiedemann, "A 1.2 GeV Damping Ring Complex for the SLC," XIIth Int. Conf. High Energy Accel's., Fermilab (1983)37. Also: J.P. Delahaye and L. Rivkin, "SLC Positron Damping Ring Optics Design," PAC, TRIUMPH (1985)1695.

[2] T.O. Raubenheimer, R. Early, T. Limberg, H. Moshammer and J. Spencer, "A Possible Redesign of SLC Damping Rings," PAC, Washington, D.C. (1993)2025.

[3] R.H. Helm, M.J. Lee, P.L. Morton and M. Sands, "Evaluation of SR Integrals," PAC, San Francisco (1973)900.

[4] T. Limberg, H. Moshammer, T. Raubenheimer, J. Spencer, R. Siemann, "Calculations of Emittance and Damping Time Effects in the SLC DRs," EPAC, Berlin (1992).

[5] G. Gross and J. Spencer, "Experience with the SLC PM Multipoles," This Conference.

[6] J.E. Spencer, "Exact Transfer Functions...," Proc. Accel. Orbit & Track. Prog's.," BNL-31761 (1982)126.